SCIENTIA
Series A: *Mathematical Sciences*, Vol. 13 (2006), 58–71
Universidad Técnica Federico Santa María
Valparaíso, Chile
ISSN 0716-8446

Numerical simulation of time-harmonic scattering problems with an optimal PML

A. Bermúdez [A], L. Hervella-Nieto [B], A. Prieto [A] and R. Rodríguez [C]

Abstract. We present an optimal bounded Perfectly Matched Layer (PML) by choosing a particular absorbing function with unbounded integral. With this choice, any spurious reflection is avoided even when the thickness of the layer is finite. We show that such choice is easy to implement in a finite element method and overcomes the dependency of parameters for the discrete problem. Finally, we presents some numerical tests.

1. Introduction

The scattering problems in unbounded domains have many practical applications. To solve numerically this kind of problems, it is necessary to truncate the computational domain, what can be done by several ways: imposing absorbing boundary conditions, using the boundary element method, Dirichlet to Neumann operators, etc. (see, for instance, (1; 8; 10)). In this work we consider an alternative approach: the so called *Perfectly Matched Layer* (PML) method, introduced by Berenger in (3).

The PML method is based on simulating an absorbing layer of damping material surrounding the domain of interest, like a thin sponge which absorbs the scattered field radiated to the exterior of this domain. It is

2000 *Mathematics Subject Classification.* Primary 65N30, 65N99 Secondary 76Q05.

Key words and phrases. Perfectly matched layer, time-harmonic scattering, Helmholtz equation .

known as 'perfectly matched' because the interface between the fluid domain and the absorbing layer does not produce spurious reflections inside the domain of interest.

In practice, since the PML has to be truncated at a finite distance of the domain of interest, its external boundary produces artificial reflections. Theoretically, these reflections are of minor importance because of the exponential decay of the acoustic waves inside the PML. In fact, for Helmholtz-type scattering problems, Lassas and Somersalo (9) proved, using boundary integral equation techniques, that the approximate solution obtained by the PML method converges exponentially to the exact solution in the computational domain as the thickness of the layer tends to infinity. This result was generalized by Hohage *et al.* (7) using techniques based on the pole condition. Similarly, Becache *et al.* (2) proved an analogous result for the convected Helmholtz equation.

When the problem is discretized, the approximation error typically gets larger, and depends on many parameters (shape of the source, physical data, discretization, etc.). Increasing the thickness of the PML may be a remedy, but not always available because of computational cost. An alternative usual choice to achieve low error levels is to take larger values for the damping function involved in the complex-valued coordinate stretching. However, Collino and Monk (6) showed that this methodology may produce an increasing error in the discretized problem. Consequently, we have to choose an optimal absorbing function to minimize the error.

In (4) we have proposed to take a damping function with unbounded integral on the PML layer. In this way, at the continuous level and with a bounded PML layer, we recover the exact solution of the original time-harmonic scattering problem stated in an unbounded domain.

The outline of this paper is as follows: In Section 2 we recall the classical two-dimensional scattering problem with Cartesian perfectly matched layers. In Section 3 we consider a special case, easy to analyze: the propagation of plane waves with oblique incidence in a 2D unbounded domain. We show that a PML method based on a non-integrable absorbing function allows recovering the exact solution in the domain of interest. In Section 4 we come back to the original PML problem to propose a finite element method to solve it. Finally, in Section 5, we report the numerical results obtained with our PML methods applied to some real-life scattering problems.

2. Cartesian PML layers

We deal with the time-harmonic scattering problem stated in an unbounded domain. More precisely, let Ω be a bounded domain in $\mathbb{R}^2$, where the obstacle of the scattering problem is situated. We assume that it has a totally reflected boundary denoted by Γ. Our goal is to solve the following problem:

For fixed frequency $\omega > 0$ and acoustic excitation g, find the pressure field p such that

$$\left\{\begin{array}{ll} \Delta p + k^2 p = 0 & \text{in } \mathbb{R}^2 \setminus \overline{\Omega}, \\ \dfrac{\partial p}{\partial \boldsymbol{n}} = g & \text{on } \Gamma, \\ \lim\limits_{|\boldsymbol{x}|\to\infty} |\boldsymbol{x}|^{\frac{1}{2}} \left(\dfrac{\partial p}{\partial |\boldsymbol{x}|} - ikp \right) = 0, & \end{array}\right. \tag{2.1}$$

where $\boldsymbol{n}$ is the unit normal vector to Γ outward to Ω and $k = \frac{\omega}{c}$ is the wave number, c being the sound speed in the physical domain.

We introduce PML layers on the x and y directions in order to truncate the unbounded domain $\mathbb{R}^2 \setminus \Omega$. With this purpose we choose a rectangular domain, $(-a, a) \times (-b, b)$, containing $\overline{\Omega}$, and a second rectangle, $(-a^\star, a^\star) \times (-b^\star, b^\star)$, containing the first one, *i.e.*, satisfying $a < a^\star$ and $b < b^\star$ (see Figure 1).

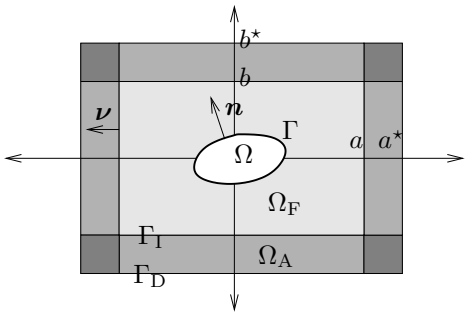

FIGURE 1. Cartesian PML layers on a two-dimensional domain.

We introduce some notation on the domains, as we show in Figure 1. We denote the physical domain by

$$\Omega_{\rm F} = [(-a, a) \times (-b, b)] \setminus \overline{\Omega},$$

whereas the bounded PML is situated in

$$\Omega_{\mathrm{A}} = [(-a^\star, a^\star) \times (-b^\star, b^\star)] \setminus [(-a, a) \times (-b, b)] .$$

The interface between the fluid cavity and the absorbing layer is denoted by $\Gamma_{\mathrm{I}} = \partial\Omega_{\mathrm{F}} \setminus \Gamma$ whereas $\Gamma_{\mathrm{D}} = \partial\Omega_{\mathrm{A}} \setminus \Gamma_{\mathrm{I}}$ denotes the artificial boundary where the perfectly matched layer is truncated. The vector $\boldsymbol{\nu} = (\nu_x, \nu_y)$ denotes the unit normal vector to Γ_{I} outward to Ω_{F}.

Since the deduction of the PML equations is nowadays well known (see, for instance, (8)), we just show the final system of equations. Given two absorbing functions, σ_x and σ_y, defined, respectively, in $[a, a^\star)$ and $[b, b^\star)$, strictly positive and not decreasing, the pressure p_{F} in the domain of interest and the pressure p_{A} in the PML are the solution of the following equations:

$$\text{(2.2)} \quad \begin{cases} \Delta p_{\mathrm{F}} + k^2 p_{\mathrm{F}} = 0 & \text{in } \Omega_{\mathrm{F}}, \\ \dfrac{1}{\gamma_x}\dfrac{\partial}{\partial x}\left(\dfrac{1}{\gamma_x}\dfrac{\partial p_{\mathrm{A}}}{\partial x}\right) + \dfrac{1}{\gamma_y}\dfrac{\partial}{\partial y}\left(\dfrac{1}{\gamma_y}\dfrac{\partial p_{\mathrm{A}}}{\partial y}\right) + k^2 p_{\mathrm{A}} = 0 & \text{in } \Omega_{\mathrm{A}}, \\ \dfrac{\partial p_{\mathrm{F}}}{\partial \boldsymbol{n}} = g & \text{on } \Gamma, \\ p_{\mathrm{F}} = p_{\mathrm{A}} & \text{on } \Gamma_{\mathrm{I}}, \\ \dfrac{\partial p_{\mathrm{F}}}{\partial \nu_x} + \dfrac{\partial p_{\mathrm{F}}}{\partial \nu_y} = \dfrac{1}{\gamma_x}\dfrac{\partial p_{\mathrm{A}}}{\partial \nu_x} + \dfrac{1}{\gamma_y}\dfrac{\partial p_{\mathrm{A}}}{\partial \nu_y} & \text{on } \Gamma_{\mathrm{I}}, \\ p_{\mathrm{A}} = 0 & \text{on } \Gamma_{\mathrm{D}}, \end{cases}$$

where

$$\gamma_x(x) = \begin{cases} 1, & x \in (a, a), \\ 1 + \frac{i}{\omega}\sigma_x(|x|), & x \in (-a^\star, -a] \cup [a, a^\star), \end{cases}$$

$$\gamma_y(y) = \begin{cases} 1, & y \in (b, b), \\ 1 + \frac{i}{\omega}\sigma_y(|y|), & y \in (-b^\star, -b] \cup [b, b^\star). \end{cases}$$

3. Plane waves with oblique incidence

In this section we deal with a particular Helmholtz problem: the propagation of two-dimensional acoustic plane waves with oblique incidence on the artificial boundary $x = 0$. This case is interesting because the original and the PML problems both can be explicitly solved, what will allow us to get a deeper knowledge about the choice of the absorbing function, which is the main goal of this work.

For a given incidence angle $\theta \in \left[0, \frac{\pi}{2}\right)$ and a wave-number k, we are interested in the following time-harmonic problem in the right-half space:

$$\begin{cases} \Delta p + k^2 p = 0 & x > 0, \\ p(0,y) = e^{ik_y y}, & \\ \lim\limits_{x\to+\infty} \left(\dfrac{\partial p}{\partial x} - ik_x p \right) = 0, & \end{cases} \tag{3.1}$$

where $k_x = k\cos\theta$ and $k_y = k\sin\theta$. It is easy to see that the solution of this problem is the plane wave $p(x,y) = e^{i(k_x x + k_y y)}$.

To truncate the physical unbounded domain in the x-direction, we introduce a PML in the horizontal strip $a < x < a^\star$. Then, we consider equations (2.2) with PML layers exclusively in the x direction (*i.e.*, $\gamma_y = 1$).

If we impose the homogeneous Dirichlet boundary condition at $x = a^\star$, $p_{\rm A}(a^\star, y) = 0$, straightforward computations leads to the analytical expression of the solution to the above PML problem is

$$\begin{cases} p_{\rm F}(x,y) = \left[(1 - R_{\rm A})\, e^{ik_x x} + R_{\rm A} e^{-ik_x x} \right] e^{ik_y y}, \\ p_{\rm A}(x,y) = \left[(1 - R_{\rm A})\, e^{ikx} e^{-\frac{1}{c}\int_a^x \sigma(s)\, ds} + R_{\rm A} e^{-ikx} e^{\frac{1}{c}\int_a^x \sigma(s)\, ds} \right] e^{ik_y y}, \end{cases} \tag{3.2}$$

where $R_{\rm A}$ is given by

$$R_{\rm A} = \frac{e^{2ik_x\, a^\star}}{e^{2ik_x\, a^\star} - \mathrm{e}^{\frac{2\cos\theta}{c}\int_a^{a^\star} \sigma_x(s)\, ds}}. \tag{3.3}$$

Since $\theta \in [0, \frac{\pi}{2})$, it is immediate to deduce from (3.3) that the larger the integral $\int_a^{a^\star} \sigma_x(s)\, ds$, the closer $R_{\rm A}$ to zero and, consequently, the closer p to $p_{\rm F}$ in the domain of interest ($0 < x < a$). Actually, if $\int_a^{a^\star} \sigma(s)\, ds < \infty$, it is easy to see that

$$\| p(\cdot, y) - p_{\rm F}(\cdot, y) \|_{L^2(0,a)} = |R_{\rm A}|\, C(k,a) \qquad \forall y \in \mathbb{R},$$

where $C(k,a) = \sqrt{\dfrac{\sin(2ka) + 2ka}{k}}$.

Classical PML techniques rely on taking a bounded absorbing function σ_x, such that its integral in $[a, a^\star]$ be sufficiently large. We propose instead to use an unbounded σ_x, such that $\int_a^{a^\star} \sigma_x(s)\, ds = +\infty$. In this case, the resulting $p_{\rm F}$ will coincide exactly with p in the domain of interest.

In order to illustrate this behavior we take the following parameters: $a = 0.5$ m, $a^\star = 0.6$ m, $\omega = 1200$ rad/s, $c = 340$ m/s, and $\theta = \frac{3\pi}{8}$ rad.

We compare two examples of the above mentioned absorbing functions: a classical choice, that is, the quadratic function taking the value $\sigma^\star$ at $x = a^\star$,

$$\sigma_x(x) = \sigma^{(\mathrm{Q})}(x) = \frac{\sigma^\star}{(a^\star - a)^2}(x-a)^2 \qquad x \in [a, a^\star), \tag{3.4}$$

and the following unbounded function with unbounded integral in $[a, a^\star)$,

$$\sigma_x(x) = \sigma^{(\mathrm{U})}(x) = \frac{c}{a^\star - x} \qquad x \in [a, a^\star). \tag{3.5}$$

In Figures 2 and 3 we can see that, when choosing the quadratic function, p_{F} approximates the exact solution p when $\sigma^\star$ becomes large. The reflection coefficient is, in this case, $R_{\mathrm{A}} = 0.26$ for $\sigma^\star = 50c$, and $R_{\mathrm{A}} = 2.88 \times 10^{-6}$ for $\sigma^\star = 500c$. In the same Figure we can see that the error is 0 when choosing the unbounded absorbing function, $\sigma^{(\mathrm{U})}$.

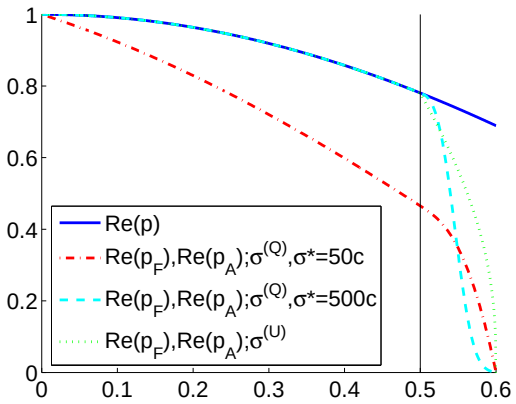

FIGURE 2. Real part of exact and approximated pressures for $\theta = 3\pi/8$.

In Figure 4 we show the dependency of the reflection coefficient R_{A}, with respect to the angle of incidence of the plane wave, when $\sigma^{(\mathrm{Q})}$ is used. It is important to emphasize that, in this case, the reflection coefficient (and hence the error) increases when taking a larger angle of incidence, whereas the error is null, for any angle of incidence, when $\sigma^{(\mathrm{U})}$ is used.

Analogously, we show, in Figure 5, the dependency of R_{A} with respect to the frequency ω when $\sigma^{(\mathrm{Q})}$ is used. For this test we have taken as angle of incidence $\theta = 0.99\frac{\pi}{2}$ (very close to the critical value $\frac{\pi}{2}$). We can observe

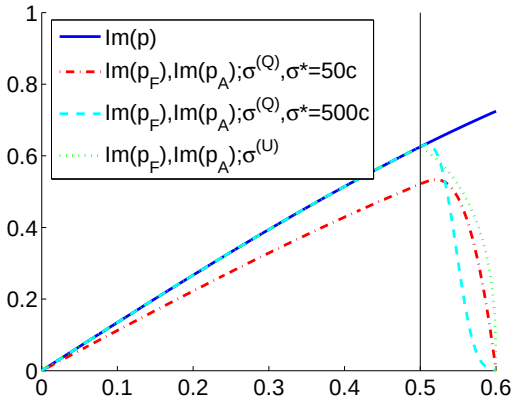

FIGURE 3. Imaginary part of exact and approximated pressures for $\theta = 3\pi/8$.

that R_{A} achieves periodically maximum values for certain frequencies. Again, we want to remark that, taking the unbounded absorbing function $\sigma^{(\mathrm{U})}$ in the PML, we recover $R_{\mathrm{A}} = 0$, for any value of the frequency.

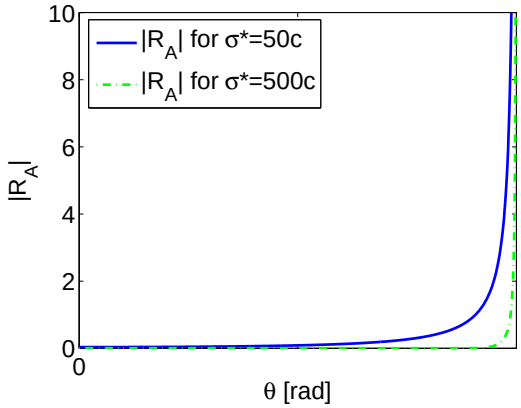

FIGURE 4. Absolute value of the reflection coefficient for $\sigma^{(\mathrm{Q})}$ versus incidence angle.

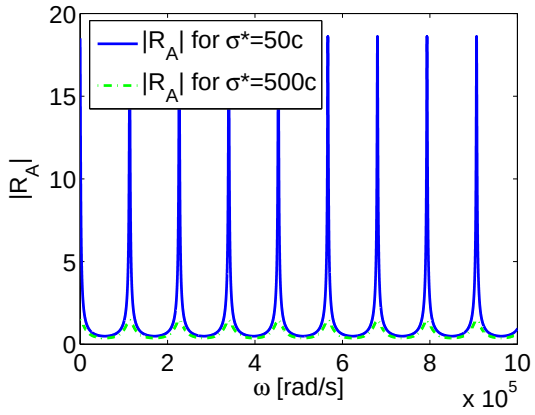

FIGURE 5. Absolute value of the reflection coefficient for $\sigma^{(\mathrm{Q})}$ versus frequency.

4. Finite element discretization

In this section we present a standard finite element method to solve the general problem (2.2). Let $\mathcal{T}_h$ be a partition of $\Omega_{\mathrm{F}} \cup \Omega_{\mathrm{A}}$ such that each element is completely contained either in Ω_{F} or in Ω_{A}. We assume that the elements in the fluid domain are triangles whereas the elements lying in the perfectly matched layer are rectangles.

We approximate the fluid pressure field, p_{F}, using continuous piecewise linear finite elements in each triangle, whereas we approximate the PML pressure field, p_{A}, using continuous piecewise bilinear Q_1 finite elements in each rectangle, vanishing on Γ_{D}.

The degrees of freedom defining the approximate pressure fields, p_{F}^h and p_{A}^h, are the values at the vertices of the triangular and rectangular meshes, respectively.

In this finite element framework, we define the following discrete problem from the weak formulation of problem (2.2):

For fixed frequency $\omega > 0$ and acoustical excitation g on Γ, find (p_F^h, p_A^h) such that

$$\begin{aligned} &\int_{\Omega_F} grad\, p_F^h \cdot grad\, \bar{q}_F^h \, dV - \int_{\Omega_F} k^2 p_F^h \bar{q}_F^h \, dV + \int_{\Omega_A} \frac{\gamma_y}{\gamma_x} \frac{\partial p_A^h}{\partial x} \frac{\partial \bar{q}_A^h}{\partial x} \, dV \\ &+ \int_{\Omega_A} \frac{\gamma_x}{\gamma_y} \frac{\partial p_A^h}{\partial y} \frac{\partial \bar{q}_A^h}{\partial y} \, dV - \int_{\Omega_A} k^2 \gamma_x \gamma_y p_F^h \bar{q}_A^h \, dV = \int_{\Gamma} g \bar{q}_F^h \, dS, \end{aligned} \tag{4.1}$$

for all discrete virtual pressure fields (q_F^h, q_A^h) *in the corresponding finite element spaces.*

5. Numerical results

In this section we study a *real life* Helmholtz problem stated in an unbounded domain using the non integrable absorbing function (3.5). More numerical examples can be found in (5).

We consider that the obstacle of the problem is a diapason whose thickness is 0.2 m, its interior aperture 1 m, and its length 4.1 m (see Figure 6).

In the first problem, we consider that a plane wave in the positive x-direction is scattered by the diapason. The mesh corresponds to the physical domain $\Omega_{\rm F} = [-3.6, 3.6]^2 \setminus \overline{\Omega}$ and to PML layers with thickness 0.5 m. We use two meshes, named mesh 4 and mesh 8, which are refinements of the mesh in Figure 6. Mesh $N = 4$ has 9140 triangles in $\Omega_{\rm F}$ and 3120 rectangles in the PML layers, whereas mesh $N = 8$ has 36610 triangles in the fluid domain and 12480 in the PML.

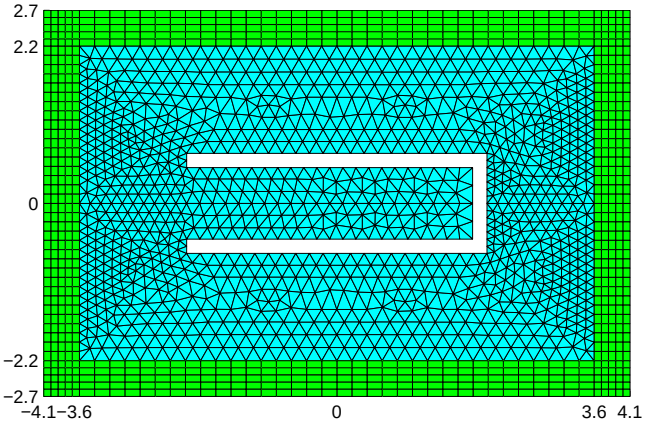

FIGURE 6. Mesh of the fluid domain and PML surrounding the diapason.

In Figures 7 and 8 we show the results that we have obtained for the reflected pressure field by the diapason, for a wave number $k = 2\pi\,\mathrm{m}^{-1}$, using the mesh $N = 4$.

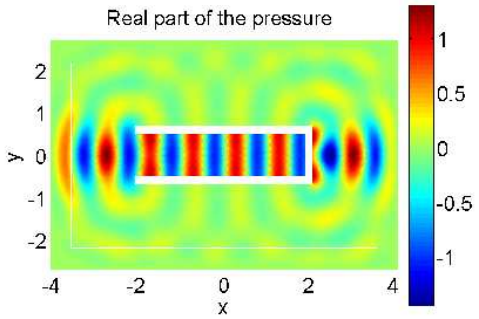

FIGURE 7. Real part of the pressure field generated by an incident plane wave, $k = 2\pi\,\mathrm{m}^{-1}$.

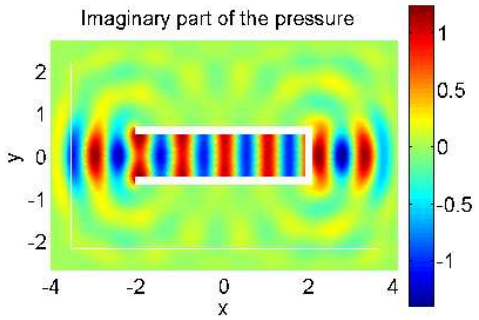

FIGURE 8. Imaginary part of the pressure field generated by an incident plane wave, $k = 2\pi\,\mathrm{m}^{-1}$.

Figures 9 and 10 show the same numerical problem with a higher wave number, $k = 10\pi\,\mathrm{m}^{-1}$. In this case we have used the mesh $N = 8$.

In the second numerical experiment we keep the same geometry and meshes, but now we simulate a Dirac's delta (monopole) actuating at the point $(0.5, 0)$ m (inside the arc of the diapason). In Figures 11–14 we show the real and the imaginary part of the reflected pressure fields generated

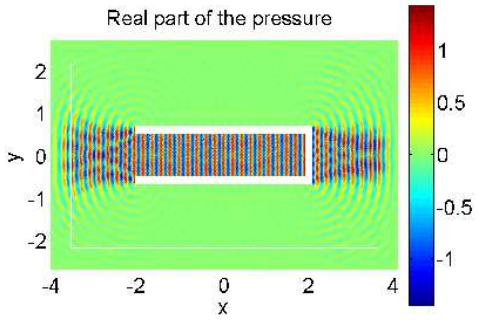

FIGURE 9. Real part of the pressure field generated by an incident plane wave, $k = 10\pi\,\mathrm{m}^{-1}$.

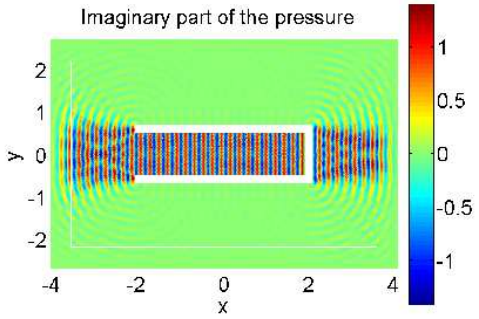

FIGURE 10. Imaginary part of the pressure field generated by an incident plane wave, $k = 10\pi\,\mathrm{m}^{-1}$.

by a monopole for the wave numbers $k = 2\pi\,\mathrm{m}^{-1}$ (with the mesh $N = 4$) and $k = 10\pi\,\mathrm{m}^{-1}$ (with the mesh $N = 8$).

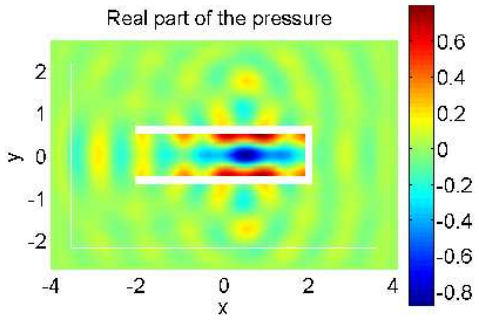

FIGURE 11. Real part of pressure field generated by a monopole, $k = 2\pi\,\mathrm{m}^{-1}$.

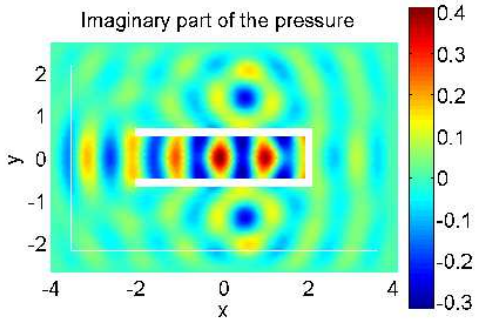

FIGURE 12. Imaginary part of the pressure field generated by a monopole, $k = 2\pi\,\mathrm{m}^{-1}$.

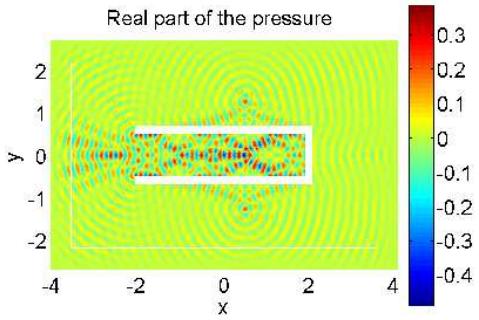

FIGURE 13. Real part of the pressure field generated by a monopole, $k = 10\pi\,\mathrm{m}^{-1}$.

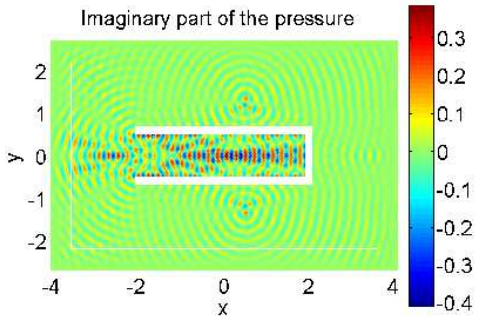

FIGURE 14. Imaginary part of the pressure field generated by a monopole, $k = 10\pi\,\mathrm{m}^{-1}$.

References

[1] R.J. Astley, Infinite elements for wave problems: A review of current formulations and an assessment of accuracy, Int. J. Numer. Methods Eng. 49 (2000) 951–976.

[2] E. Bécache, A.-S. Bonnet-Benn Dhia, G. Legendre, Perfectly matched layer for the convected Helmholtz equation, SIAM J. Numer. Anal. 42 (2004) 409–433.

[3] J.P. Berenger, A perfectly matched layer for the absorption of electromagnetic waves, J. Comput. Phys. 114 (1994) 185–200.

[4] A. Bermúdez, L.M. Hervella-Nieto, A. Prieto, R. Rodríguez, An exact bounded PML for the Helmholtz equation, C. R. Acad. Sci. Paris, Ser. I, Math. 339 (2004) 803–808.
[5] A. Bermúdez, L.M. Hervella-Nieto, A. Prieto, R. Rodríguez, An optimal perfectly matched layer with unbounded absorbing function for time-harmonic acoustic scattering problems.(submitted).
[6] F. Collino, P. Monk, Optimizing the perfectly matched layer, Comput. Methods Appl. Mech. Eng. 164 (1998) 157–171.
[7] T. Hohage, F. Schmidt, L. Zschiedrich, Solving time-harmonic scattering problems based on the pole condition II: convergence of the PML method, SIAM J. Math. Anal. 35 (2003) 547–560.
[8] F. Ihlenburg, Finite Element of Analysis of Acoustical Scattering, Springer-Verlag, New York, 1998.
[9] M. Lassas, E. Somersalo, On the existence and convergence of the solution of PML equations, Computing, 60 (1998) 228–241.
[10] J.-C.Nédélec, Acoustic and Electromagnetic Equations. Integral Representations for Harmonic Problems, Springer-Verlag, New York, 2000.

Received 10 05 2006, revised 18 08 2006

[A]Departamento de Matemática Aplicada,
Universidade de Santiago de Compostela,
15706 - Santiago de Compostela, Spain.
E-mail address: mabermud@usc.es, maprieto@usc.es

[B]Departamento de Matemática,
Universidade da Coruña,
15071 - A Coruña, Spain.
E-mail address: luisher@udc.es

[C]Departamento de Ingeniería Matemática,
Universidad de Concepción,
Casilla 160-C,
Concepción, Chile.
E-mail address: rodolfo@ing-mat.udec.cl